Molecules and Cells

Combination Therapy with a PI3K/mTOR Dual Inhibitor and Chloroquine Enhances Synergistic Apoptotic Cell Death in Epstein–Barr Virus-Infected Gastric Cancer Cells

Mi-Young Kim[1,2,*], Annie J. Kruger[2,3], Ju-Yeon Jeong[4], Jaehee Kim[4], Phil kyung Shin[4], Sun Young Kim[5], Joo Young Cho[1], Ki Baik Hahm[1], and Sung Pyo Hong[1]

[1]Digestive Disease Center, [4]Institute for Clinical Research, CHA Bundang Medical Center, CHA University, Seongnam 13496, Korea, [2]Liver Center and Gastrointestinal Division, Department of Medicine, Massachusetts General Hospital, Harvard Medical School, Boston, MA 02114, USA, [3]Division of Gastroenterology, MedStar Georgetown University Hospital, Washington, DC 20007, USA, [5]Department of Hematology and Oncology, Samsung Medical Center, Sungkyunkwan University School of Medicine, Seoul 06351, Korea
*Correspondence: mykim@cha.ac.kr
https://doi.org/10.14348/molcells.2019.2395
www.molcells.org

The phosphoinositide 3-kinase/protein kinase B/mammalian target of rapamycin (PI3K/AKT/mTOR) signaling pathway is a promising target for gastric cancer (GC) treatment; however the efficacy of PI3K/mTOR dual inhibitors in GC has not yet been maximized. Additionally, the effect of autophagy regulation by PI3K/mTOR dual inhibitors has not been clearly elucidated in GC treatment. We aimed to show that our newly developed PI3K/mTOR dual inhibitor, CMG002, when combined with an autophagy inhibitor, chloroquine (CQ), potently induces effective cancer cell death in Epstein-Barr virus (EBV)-associated gastric cancer (EBVaGC) cells, where both the PI3K/AKT/mTOR and autophagy pathways play important roles in disease pathogenesis. EBV- and mock-infected AGS and NUGC3 GC cell lines were treated with CMG002 +/− CQ. PI3K/AKT/mTOR signaling pathway mediators, cellular apoptosis and autophagy markers were confirmed by Western blot assay. Cell viability was assessed using the Cell Counting Kit-8 (CCK-8) assay. CMG002 effectively blocked the PI3K/AKT/mTOR pathway by markedly decreasing phosphorylation of AKT and its downstream mediator S6. CMG002 induced G0/G1 cell cycle arrest and enhanced apoptotic cell death in AGS and NUGC3 cells, particularly EBV-infected cells compared with mock-infected cells, as confirmed by flow cytometric analyses and TUNEL (terminal deoxynucleotidyl transferase dUTP nick end labeling) assays. The combination of CMG002 plus CQ synergistically increased apoptotic cell death in EBV-infected GC cell lines when compared with CMG002 alone ($P < 0.05$). Our results suggest that the new PI3K/mTOR dual inhibitor, CMG002, when used in combination with the autophagy inhibitor, CQ, provides enhanced therapeutic efficacy against EBVaGC.

Keywords: apoptosis, autophagy, chloroquine, gastric cancer, PI3K/mTOR dual inhibitor

INTRODUCTION

The phosphoinositide 3-kinase/protein kinase B/mammalian

Received 22 September, 2018; revised 26 March, 2019; accepted 27 March, 2019; published online 3 May, 2019

eISSN: 0219-1032

target of rapamycin (PI3K/AKT/mTOR) signaling pathway harbors important targets for gastric cancer (GC) treatment since activation of PI3K and its downstream mediator, AKT, is frequently observed in GC, often associated with the oncogenic *PIK3CA* mutation or loss of function of *PTEN* tumor suppressor gene (Samuels et al., 2004). Activation of the PI3K/AKT/mTOR pathway not only enhances carcinogenesis by promoting cell growth, cell cycle dysregulation and cell survival, but also contributes to cancer metastasis, chemotherapeutic resistance and recurrence (Fang et al., 2016; Liu et al., 2014; Shin et al., 2010). Recently, the importance of the PI3K/AKT/mTOR pathway activation in influencing treatment response to GC became particularly pertinent. In human epidermal growth factor (HER2)-positive GC, the therapeutic effect of trastuzumab, a monoclonal antibody that interferes with the HER2/*neu* receptor, was reported to be lower than in breast cancer (Zhu et al., 2015), an effect directly attributed to the enhanced PI3K/AKT/mTOR signaling in GC than in breast cancer. Dual inhibition of PI3K/mTOR has been reported to enhance the response of conventional chemotherapeutic agents in the treatment of GC (Zhang et al., 2013; Zhu et al., 2015). However, GC treatment strategies that maximize the efficacy of PI3K/mTOR dual inhibitors remain limited.

PI3K/mTOR dual inhibitors can affect cell death in various cancers by influencing autophagy regulation (Mirzoeva et al., 2011). The induction of autophagy can prevent carcinogenesis by breaking down damaged cells, but could paradoxically contribute to cancer cell growth by providing nutrients for cancer cell survival (Levine and Kroemer, 2008). In gastric carcinogenesis, the functional role of autophagy in influencing cancer cell survival or cell death has not been fully described. Recently, combination therapy with autophagy inhibitors and PI3K/mTOR dual inhibitors has been reported to increase apoptotic cell death in various cancers (Chang et al., 2013; Fei et al., 2016). However, the effects of autophagy regulation by PI3K/mTOR dual inhibitors on GC cell death are poorly understood. We hypothesized that PI3K/mTOR dual inhibitor therapy could enhance apoptotic cell death in GC cell lines when combined with autophagy inhibitors.

Epstein-Barr virus (EBV)-associated GC (EBVaGC) is the most common EBV-associated cancer, accounting for about 10% of all GCs (Shibata and Weiss, 1992). The main EBV oncoproteins, latent membrane protein (LMP) 1 and LMP2A, are known inducers of carcinogenesis in EBVaGC via PI3K/AKT activation (Dawson et al., 2003; Hino et al., 2009). Therefore, we hypothesized that targeting the PI3K/AKT/mTOR signaling pathway would have a significant therapeutic benefit against EBVaGC.

In this study, we aimed to dissect the anti-cancer effects of our newly synthesized PI3K/mTOR dual inhibitor, CMG002, against EBVaGC. We have determined that CMG002 more potently induces apoptotic cell death in EBV-infected GC cell lines than non-infected GC cell lines. We additionally found that combining a PI3K/mTOR dual inhibitor with the autophagy inhibitor, chloroquine (CQ), augments apoptotic cell death in EBVaGC cell lines.

MATERIALS AND METHODS

Generation of EBV-infected GC cell lines

The AGS (ATCC: CRL-1739) and NUGC3 cell lines (Akiyama et al., 1988) were maintained in RPMI 1640 (Welgene, Korea) and DMEM (Welgene) medium supplemented with 10% fetal bovine serum (FBS; Welgene), respectively, and were infected with EBV released from Akata-BX1 cells, kindly provided by Dr. Lindsey Hutt-Fletcher (Louisiana State University, USA), as follows: EBV-GFP-infected Akata-BX1 cells were induced to undergo lytic EBV replication by cross-linking their surface immunoglobulin G (IgG) receptors with anti-IgG antibodies (Imai et al., 1998). AGS and NUGC3 cells were seeded into 12-well culture plates at a density of 2.5×10^4 cells/ml and grown to confluence. Akata-BX1 cells (5×10^5/ml) expressing surface IgG receptors cross-linked using anti-human IgG goat serum (50 μg/ml; Thermo Scientific, Waltham, MA, USA) were added to AGS and NUGC3 cells and co-cultured 3 days with replacement of half the growth media with fresh media on day 2. Following EBV infection (day 3), cells were washed four times with phosphate buffered saline (PBS) to remove residual viable virus donor cells. EBV-infected AGS and NUGC3 cells were identified 72 hours later by GFP expression, and cells harboring EBV were selected using media containing G418 (Gibco, USA), an antibiotic used for cell selection, per the manufacturer's protocol.

Chemicals

The compound CMG002, a new PI3K/mTOR dual inhibitor as a pyridopyrimidine derivative (molecular weight 617; Fig. 1) which inhibits all catalytic isoforms of PI3K (p110α, β, γ, and δ) and mTORC1/2, was provided by CMG Pharmaceutical (Dr. Jeong Beob Seo, CMG Pharmaceutical, Korea). It was dissolved in PBS and stored at –20°C until rapidly thawed to room temperature for each experiment.

Reverse transcription polymerase chain reaction

Total RNA was extracted using TRIzol (Invitrogen, USA). cDNA was generated from 1 μg of purified total RNA from each sample using SuperScript II reverse transcriptase (Invitrogen).

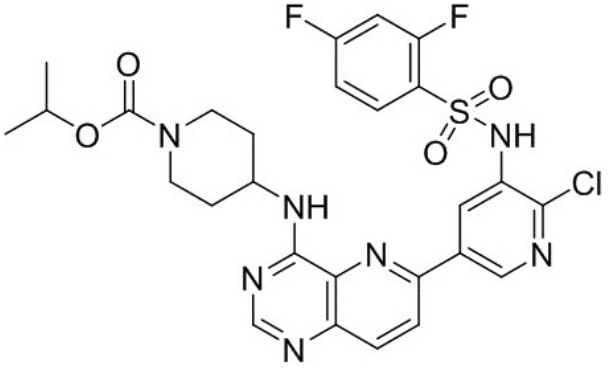

Fig. 1. Chemical structure of CMG002, Isopropyl 4-(6-(6-chloro-5-(2,4-difluorophenylsulfonamido)pyridine-3-yl)pyrido[3,2-*d*]pyrimidin-4-ylamino)piperidine-1-carboxylate.

Table 1. Information on primers for PCR

Gene	Forward primer (5'-3')	Reverse primer (5'-3')	Size (bp)
EBNA1	AGATGACCCAGGAGAAGGCCCAAGC	CAAAGGGGAGACGACTCAATG	308
GAPDH	CACTGGCGTCTTCACCACCATG	GCTTCACCACCTTCTTGATGTCA	465

The polymerase chain reaction (PCR) amplification was performed using 2× PCR Master mix solution (AccuPower PCRPreMix; Bioneer, Korea) with appropriate cycles. Forward and reverse PCR primers used in this study are described in Table 1.

Western blotting

Cells were lysed on ice in PRO-PREP protein extraction solution (iNtRON Biotechnology, Korea) containing 10× PhosSTOP Phosphatase inhibitor cocktail tablets (Roche, Switzerland). The protein concentration was analyzed by Pierce BCA protein assay kit (Thermo Scientific, Rockford, IL, USA). The protein samples (20 μg/lane) were separated on 12% SDS-PAGE gel and transferred onto nitrocellulose-membranes (Bio-Rad, USA) and blocked with 4% to 5% non-fat dry milk in TBS containing 0.1% Tween-20 for 1 hour. After blocking, the membranes were subjected to western blotting with primary antibodies against Epstein-Barr nuclear antigen1 (EBNA1) (#sc-81581; Santa Cruz Biotechnology, USA); poly (ADP-ribose) polymerase 1 (PARP-1) (#sc-7150; Santa Cruz Biotechnology); β-actin (#sc-47778; Santa Cruz Biotechnology); Akt (#9272s; Cell Signaling Technology [CST], USA); phospho-Akt (Ser473) (#9271s; CST); extracellular signal-regulated kinase1/2 (Erk1/2) (#4695s; CST); phospho-p44/42 MAPK (Erk1/2) (Thr202/Tyr204) (#4370s; CST); S6 ribosomal protein (#2217s; CST); cleaved caspase-3 (#9664; CST); caspase-3 (#9662; CST); light chain 3B (LC3B) (#2775; CST); and glyceraldehyde 3-phosphate dehydrogenase (GAPDH) (#97166; CST) incubated at 4°C overnight. The secondary antibodies used were goat anti-mouse IgG (H + L) (#1706516; Bio-Rad) or goat anti-rabbit IgG (H + L) (#1706515; Bio-Rad). Immunoreactive bands were detected using the Clarity Western ECL Substrate kit (Bio-Rad). Chemiluminescence signals were detected using the ChemiDOC XRS + system (Bio-Rad).

Cell viability assay

Cell proliferation and cytotoxicity was assessed using the Cell Counting Kit-8 (CCK-8; Dojindo Molecular Technologies, USA) assay. Briefly, 5×10^3 cells per well were seeded onto 96-well plates. Treatment (CMG002 and/or CQ) was added 24 hours after cell seeding, and the cells were incubated for 48 hours. Cell viability was checked in drug-treated and untreated cells using CCK-8, which was added to each well and incubated for 3 hours. The optical densities were measured at 450 nm with a microplate analyzer. The results represent the mean of five wells, and all experiments were performed in triplicate.

Cell cycle analysis

The cell cycle was analyzed by flow cytometry. Briefly, 1×10^6 cells were collected and washed in PBS, then fixed in 75% alcohol for 1 hour at -20°C. After washing in cold PBS three times, cells were resuspended in 500 μl of PI/RNase staining buffer (BD Bioscience, USA) and incubated for 15 minutes at 37°C in the dark. Samples were then analyzed for their DNA content by fluorescence activated cell sorting (FACS, Becton Dickinson, USA). Each experiment was performed in triplicate.

TUNEL assay

Apoptotic cells were analyzed using the *In Situ* Cell Death Detection kit (Roche, Germany). Cells (2×10^7) were fixed with 75% ethanol for 2 hours at –20°C, washed twice with PBS, incubated in 0.1% Triton X-100 with 0.1% sodium citrate for 2 minutes on ice, washed twice with PBS, and incubated with a TUNEL labeling mixture for 1 hour at 37°C in the dark. The samples were washed twice with PBS and analyzed by FACS (Becton Dickinson). Each experiment was performed in triplicate.

Statistical analysis

Experiments were performed in triplicate and all results are represented as the mean ± standard error of the mean (SEM). Differences between groups were tested by one-way ANOVA followed by Duncan's multiple comparison tests with $P < 0.05$ as the criterion for significance. Data were analyzed using IBM SPSS (ver. 24.0; IBM, USA).

RESULTS

GC cell lines express EBV protein and phosphorylated AKT

To confirm EBV infection in the AGS and NUGC3 GC cell lines, *EBNA1* gene expression and EBNA1 protein levels were quantified by PCR and Western blot, respectively (Fig. 2A). RT-PCR using unique primers detected *EBNA1* mRNA in EBV-infected AGS and NUGC3 cells compared with mock-infected cells. EBNA1 protein was also detected in EBV-infected cell lines by Western blot assay. EBV-infected AGS and NUGC3 cells expressed significantly more phosphorylated AKT despite no difference in the total AKT levels between EBV- and mock-infected cells ($P < 0.001$; Fig. 2B), representing activation of the AKT signaling pathway in EBV-infected cells.

CMG002 has anti-proliferative effect in GC cell lines

We assessed the anti-proliferative effect of CMG002 in the AGS and NUGC3 cell lines using a 10-dimensional drug response assay (Fig. 3A). In both cell lines, inhibitory concentration 50 (IC_{50}) value for CMG002 was lower in EBV-infected cells than mock-infected cells. In the AGS and NUGC3 cell lines, the IC_{50} value for CMG002 was as follows: 1,564 nM (AGS, mock-infected), 1,188 nM (AGS, EBV-infected), 4,904 nM (NUGC3, mock-infected), and 3,930 nM (NUGC3, EBV-infected). To find the minimum

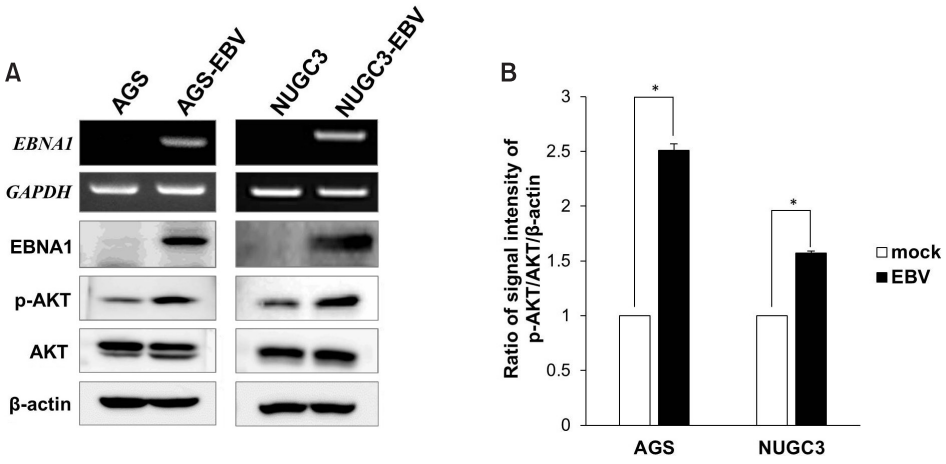

Fig. 2. Confirmation of Epstein-Barr virus (EBV) infection and its effect on phosphorylation of AKT in EBV-infected gastric cancer cell lines. (A) *Epstein-Barr nuclear antigen 1* (*EBNA1*) mRNA was detected by RT-PCR (upper 2 panels). EBNA1, p-AKT and AKT protein was detected by Western blot, respectively. Western blot data represent experiments that were performed in triplicate with EBV- and mock-infected AGS and NUGC3 cells. (B) Western blot image quantification of p-AKT to AKT ratio in EBV- and mock-infected AGS and NUGC3 cells. The data are expressed as the mean ± SEM of assays run in triplicate. $*P < 0.001$.

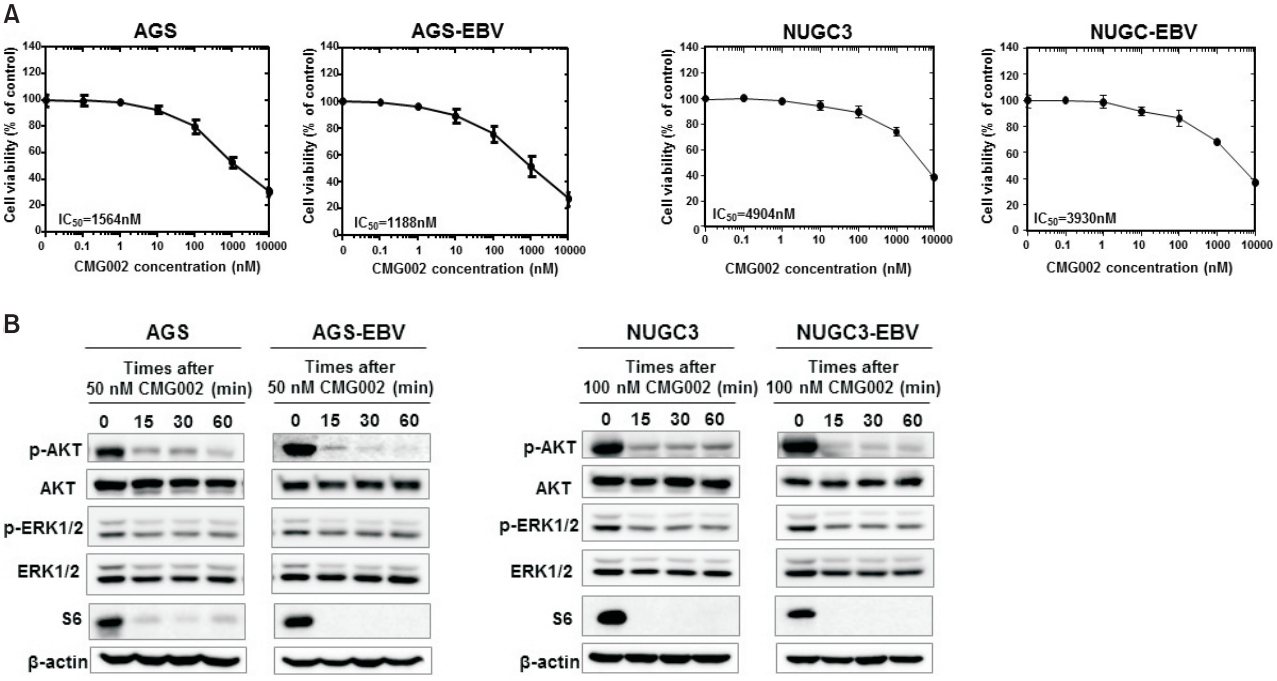

Fig. 3. Effect of CMG002 on cell viability and downstream mediators of the PI3K/AKT/mTOR pathway in EBV- and mock-infected AGS and NUGC3 cells. (A) Cell viability following CMG002 treatment assessed using a 10-dimensional drug response assay. Cells were seeded at 5×10^3 per well in 96-well culture plates, and incubated for 48 hours with CMG002, following which cell viability was performed in triplicate. Results are expressed as the mean ± SEM. (B) Western blot analysis of the PI3K/AKT/mTOR pathway proteins from AGS and NUGC3 cells 1 hour post-treatment with 50 nM and 100 nM of CMG002, respectively. Western blot data represent experiments performed in triplicate.

dose of CMG002 that resulted in a therapeutic effect, the phosphorylation status of proteins in the PI3K/AKT/mTOR signaling pathway was evaluated over 60 minutes following CMG002 treatment at concentrations of 50 nM in AGS and 100 nM in NUGC3 cells based on their IC_{50} values. Sixty minutes post-treatment, phosphorylated AKT decreased to less than 30% of pre-treatment value, consistent with the expected effects of PI3K/mTOR dual inhibition (Fig. 3B).

Interestingly, total S6, the protein downstream of mTOR, which also decreased consistently, became less than 10% of pre-treatment values within 60 minutes of CMG002 treatment in both cell lines. We were concerned that blockade of the PI3K/AKT/mTOR pathway could shunt the cellular response toward a compensatory activation of the mitogen-activated protein kinase kinase/extracellular signal-regulated kinase (MEK/ERK) pathway based on similar reports from other PI3K/mTOR dual inhibitors (Ning et al., 2017; Soares et al., 2015); however, we did not observe increased ERK phosphorylation after 60 minutes of treatment with CMG002 in either AGS or NUGC3 cells, regardless of EBV infection (Fig. 3B). To confirm that CMG002 did not have a dose-dependent effect on ERK phosphorylation, we tested a dose range of CMG002 on AGS and NUGC3 cells for 60 minutes. We found that CMG002 has no significant effect in activation of ERK at the tested concentrations, as demonstrated by a steady ratio of phosphorylated to total ERK (Supplementary Fig. S1).

CMG002 induces cell growth inhibition and cell cycle arrest

To examine the growth inhibitory effect of CMG002, AGS and NUGC3 cells were incubated with 100 nM of CMG002 for 48 hours based on the IC_{50} analysis (Fig. 3A). We used a higher, 100 nM concentration of CMG002 on AGS cells, regardless of EBV infection, because there was no growth inhibition at the lower dose of CMG002 (50 nM) in this cell

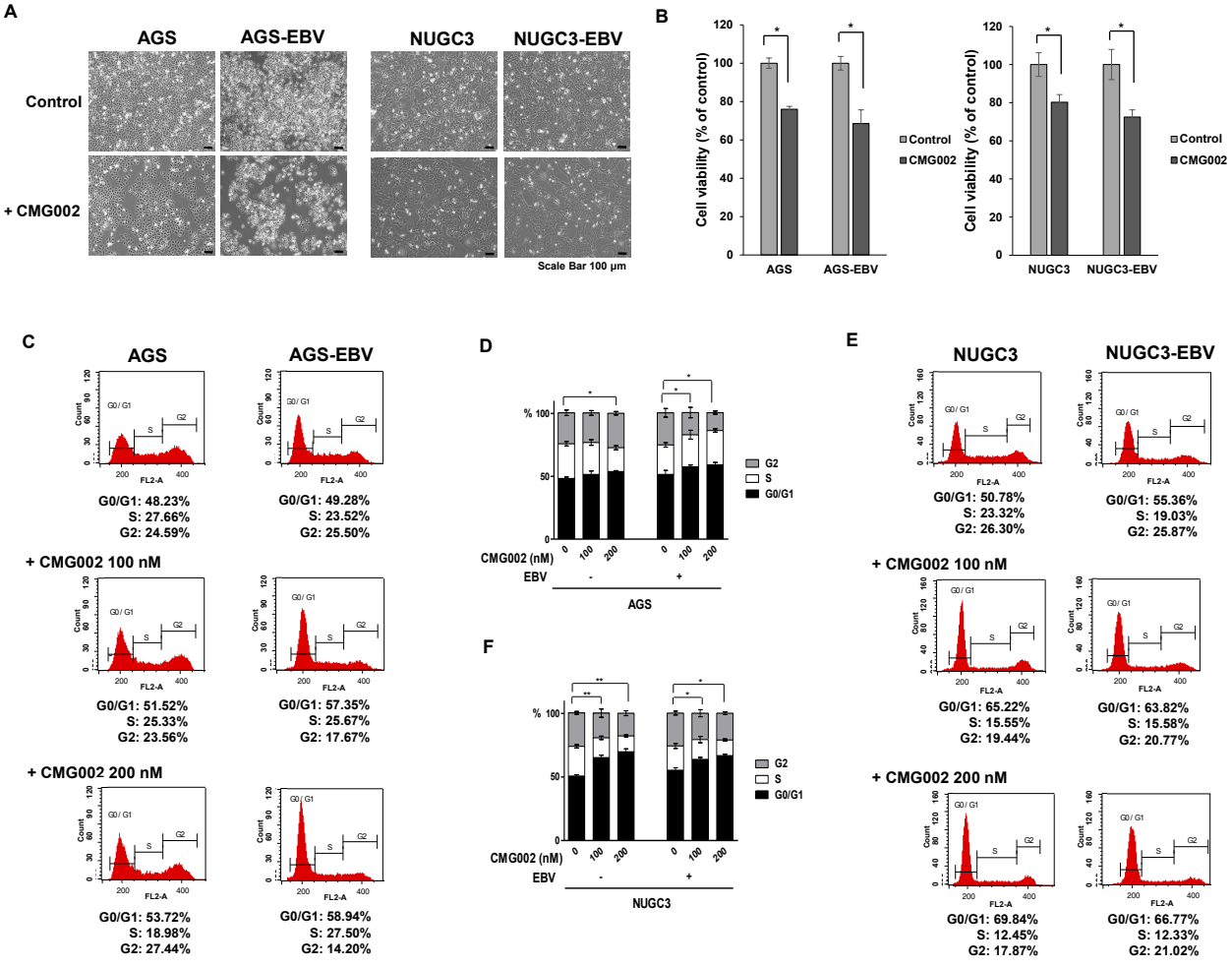

Fig. 4. CMG002 exerts its anti-proliferative effect on gastric cancer cell lines by inducing cell cycle arrest in the G0/G1 phase. (A) Representative images of AGS (left two panels) and NUGC3 (right two panels) cells treated for 48 hours with CMG002 (40× magnification). (B) CCK-8 assay-based cell viability analysis of EBV- and mock- infected AGS (left panel) and NUGC3 (right panel) cells treated for 48 hours with CMG002 compared with control cells. (C) Flow cytometry-based cell cycle analysis of CMG002 in EBV- and mock-infected AGS cells. Cells were incubated for 48 hours with CMG002 at each concentration prior to cell cycle analysis. (D) Numeric representation of changes in fraction of AGS cells in each cell cycle phase following treatment with CMG002. (E) Flow cytometry-based cell cycle analysis of CMG002 in EBV- and mock-infected NUGC3 cells. Cells were incubated for 48 hours with CMG002 at each concentration prior to cell cycle analysis. (F) Numeric representation of changes in the fraction of EBV- and mock-infected NUGC3 cells in each cell cycle phase following treatment with CMG002. Cell cycle analyses in Figures 4C and 4E were performed in triplicate and data in Figures 4D and 4F are expressed as the mean ± SEM. $*P < 0.05$; $**P < 0.001$.

line (data not shown). After 48 hours, 100 nM of CMG002 visibly affected the cell growth in AGS and NUGC3 cells (Fig. 4A), and significantly decreased cell viability in each cell line regardless of EBV infection ($P < 0.05$; Fig. 4B). Cell cycle analyses were performed to elucidate the stage where CMG002 exerted its inhibitory effect on cell proliferation (Figs. 4C and 4E). In EBV-infected AGS cells, CMG002 promoted G0/G1 arrest at much lower concentrations (100 nM) compared with mock-infected cells, which required 200 nM of CMG002 treatment to induce G0/G1 arrest ($P < 0.05$; Figs. 4C and 4D). The frequency of EBV-infected AGS cells remaining arrested in G0/G1 cycle increased from 49% to 57% following 100 nM of CMG002 treatment. In the NUGC3 cell line, G0/G1 arrest occurred in a dose-dependent fashion (100 nM vs 200 nM), irrespective of EBV infection, but the difference between infected and uninfected cells was not statistically significant (Figs. 4E and 4F). Among NUGC3 cells treated with 100 nM of CMG002, the frequency of cells arrested in G0/G1 increased significantly from 55% to 64% in EBV-infected cells ($P < 0.05$) and from 51% to 65% in mock-infected cells ($P < 0.001$), respectively.

CMG002 induces autophagy which is inhibited by CQ

The influence of PI3K/mTOR dual inhibitors on autophagy regulation is not well known in GC treatment. We were concerned that the potential autophagy-promoting effects of CMG002 may paradoxically enhance cancer cell growth, therefore, we examined the effects of CMG002 on autophagy in GC cell lines. Autophagy induction by CMG002 treatment was assessed by observing the LC3B conversion from LC3B-I to LC3B-II, which was quantified as the LC3B-II/LC3B-I ratio. When AGS and NUGC3 cell lines were incubated with CMG002 for 48 hours, LC3B-I to LC3B-II conversion was most dominantly observed in AGS cell lines ($P < 0.05$; Figs. 5A and 5B). Not only did the ratio of LC3B-II/LC3B-I increase in a dose-dependent fashion with increasing concentrations of CMG002, this ratio was more prominent in EBV-infected AGS cells than mock-infected cells. The NUGC3 cell line did not demonstrate significant activation of the autophagy pathway in response to CMG002 regardless of EBV infection because these cells appeared to have high autophagy activity at baseline. The concern for autophagy induction by CMG002 paradoxically contributing to cancer cell growth prompted us to next test the effect of inhibiting the autophagy pathway using an autophagy inhibitor, CQ. CQ is a commonly utilized late phase autophagy inhibitor which blocks the fusion of autophagosomes with lysosomes and promotes the accumulation of LC3B-II (Klionsky et al., 2016). We first confirmed that CQ did not have any independent cytotoxic effects on the AGS and NUGC3 cell lines by assessing cell viability at escalating doses of CQ using the CCK-8 assay (Fig. 5C). To avoid the potential confounding effect of CQ-induced cytotoxicity, we used a low treatment concentration of CQ, 10 μM, to examine the inhibitory effect

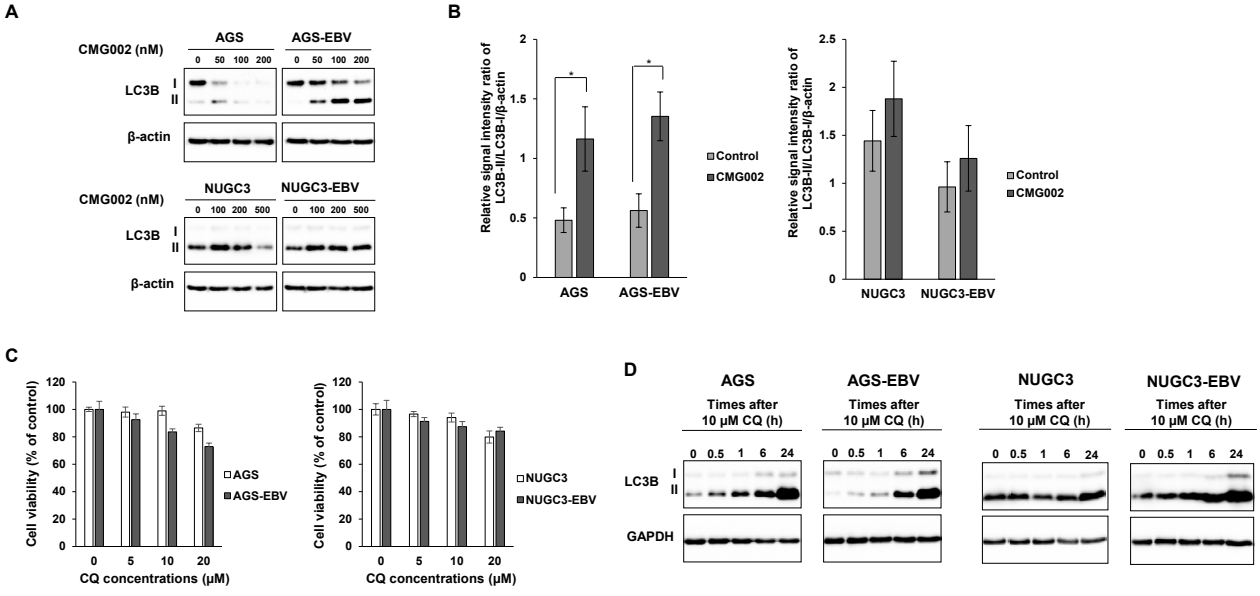

Fig. 5. Autophagy regulation by CMG002 and CQ. (A) Western blot analysis of LC3B 48 hours following increasing doses of CMG002 in EBV- and mock-infected AGS and NUGC3 cells. Western blot data represent experiments performed in triplicate. (B) Quantification of the LC3B-II to LC3B-I ratio in CMG002 treated cells compared with control cells in EBV- and mock-infected AGS (left panel) and NUGC3 (right panel) cells. Data represent experiments performed in triplicate and are expressed as the mean ± SEM. (C) CCK-8 assay-based cell viability following CQ treatment in EBV- and mock-infected AGS (left panel) and NUGC3 (right panel) cells. Cells were seeded at 5×10^3 per well in 96-well culture plates, and incubated for 48 hours with CQ treatment following which cell viability was performed in triplicate. Results expressed represent the mean ± SEM. (D) Western blot analysis of LC3B 24 hours post-treatment with 10 μM of CQ on EBV- and mock-infected AGS (left two panels) and NUGC3 (right two panels) cell lines. Western blot data represent experiments that were performed in triplicate. $*P < 0.05$.

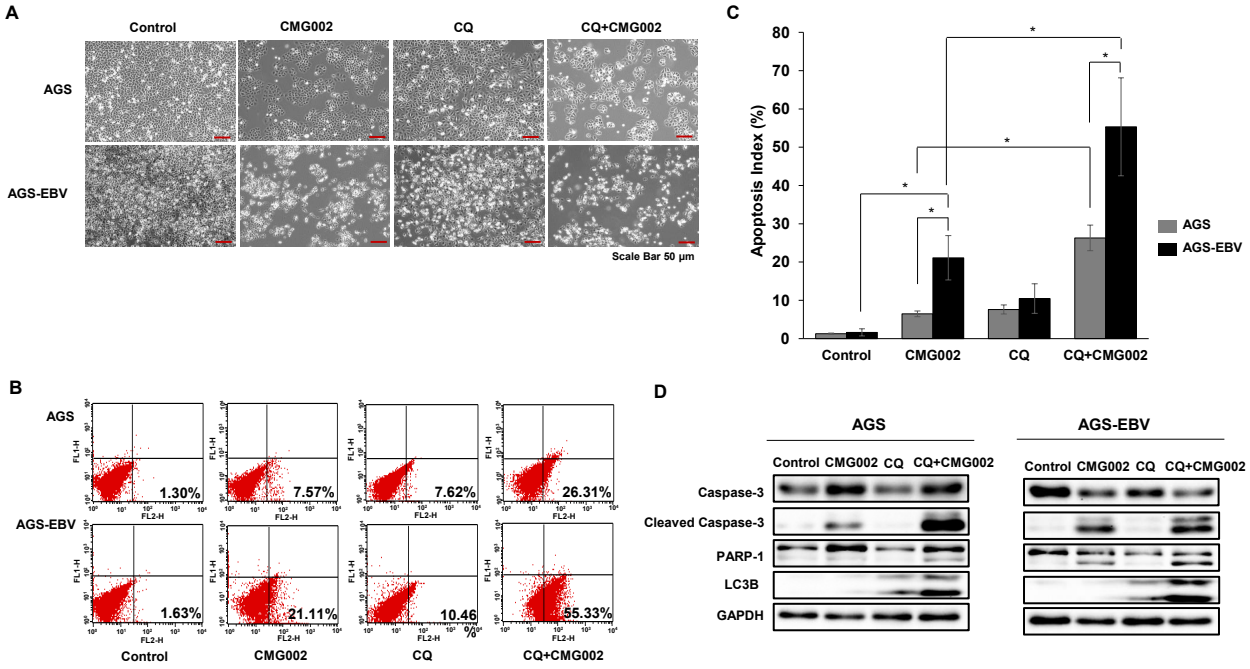

Fig. 6. Synergistic apoptotic cell death after SCT with CQ and CMG002 in AGS cell line. (A) Representative images of EBV- and mock-infected AGS cells 48 hours post-sequential combination therapy (SCT; cells were incubated with 10 μM CQ for 1 hour followed by concomitant 10 μM CQ and 100 nM of CMG002 for the remainder of the 48-hour period) (40× magnification). (B) Flow cytometry-based TUNEL assay demonstrating gating of apoptotic cells 48 hours following monotherapy and SCT. The percentage of apoptotic cells represents the mean of more than three independent experiments. (C) Apoptotic index (%) in EBV- and mock-infected AGS cells after 48 hours of treatment with CQ and CMG002 monotherapy and SCT. Results expressed represent the mean ± SEM from experiments performed in triplicate. (D) Western blot analysis of the apoptotic marker proteins, caspase-3 and PARP-1, and the autophagy marker LC3B. Western blot data represent experiments performed in triplicate. $*P < 0.05$.

of this drug on autophagy. LC3B-II accumulation increased in a time-dependent manner for up to 24 hours, regardless of EBV infection status, indicating increased autophagy inhibition in CQ treated cells (Fig. 5D).

Sequential combination therapy with CQ and CMG002 induces synergistic apoptotic cell death

To verify the effect of combination therapy with CQ and CMG002 on apoptotic cell death, experiments were performed on three groups. Cells were incubated for 48 hours with (1) CMG002 alone, (2) CQ alone, and (3) sequential therapy with pre-treatment of cells with CQ for 1 hour followed by concomitant CQ and CMG002 for the remainder of the 48-hour treatment duration, heretofore referred to as sequential combination therapy (SCT). We found that SCT inhibited cell proliferation in EBV- and mock-infected AGS cells when compared with control and CMG002 alone treated groups (Fig. 6A). We performed TUNEL assays to identify the effects of CMG002 alone and SCT on apoptotic cell death. We confirmed that SCT not only induced greater apoptotic cell death irrespective of EBV infection, but EBV-infected AGS cells were particularly susceptible to SCT ($P < 0.05$; Fig. 6B and 6C). We also found that CMG002 alone significantly increased apoptosis in EBV-infected AGS cells compared with mock-infected cells ($P < 0.05$). The effects of SCT and CMG002 alone on apoptosis and autophagy were confirmed by Western blot assay (Fig. 6D). The expression of cleaved forms of apoptotic marker proteins, caspase-3 and PARP-1, was significantly higher in the SCT group compared with CMG002 alone or controls. Similarly, SCT induced significant synergistic apoptosis in NUGC3 cells irrespective of EBV infection, but most effectively in EBV-infected cells (Fig. 7). To demonstrate that substitution of another autophagy inhibitor like bafilomycin A1 could reproduce the effect of SCT on apoptotic cell death induction in GC cell lines, we repeated the SCT experiments using bafilomycin A1 in combination with CMG002. Cells were incubated for 48 hours with (1) CMG002 alone, (2) bafilomycin A1 alone, and (3) SCT with pre-treatment of cells with bafilomycin A1 for 1 hour followed by concomitant bafilomycin A1 and CMG002 for the remainder of the 48-hour treatment duration. We confirmed that SCT with bafilomycin A1 and CMG002, like SCT with CQ and CMG002, induced synergistic apoptotic cell death in AGS and NUGC3 cell lines, particularly EBV-infected AGS and NUGC3 cells (Figs. 8 and 9).

DISCUSSION

In this study we assessed the therapeutic effect of CMG002 in blocking the PI3K/AKT/mTOR pathway, specifically PI3K and its downstream protein, AKT, in highly proliferative GC cell lines, with or without concomitant EBV infection. The

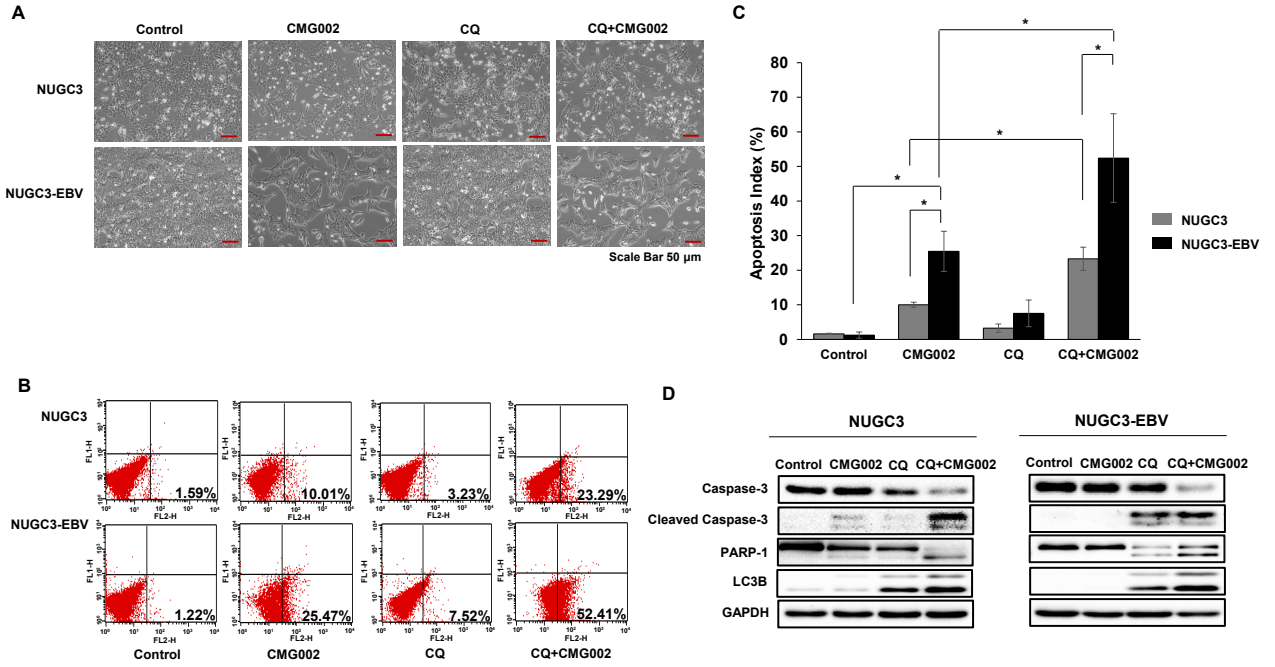

Fig. 7. Synergistic apoptotic cell death induced by SCT with CQ and CMG002 in NUGC3 cell line. (A) Representative images of EBV- and mock-infected NUGC3 cells 48 hours post-SCT with CQ and CMG002 (40× magnification). (B) Flow cytometry-based TUNEL assay demonstrating gating of apoptotic cells 48 hours following monotherapy and SCT. The percentages of apoptotic cells represent the mean of more than three independent experiments. (C) Apoptotic index (%) in EBV- and mock-infected NUGC3 cells after 48 hours of treatment with monotherapy and SCT. Results expressed represent the mean ± SEM from the experiments conducted in triplicate. (D) Western blot analysis of the apoptotic marker proteins, caspase-3 and PARP-1, and the autophagy marker LC3B. Western blot data represent experiments performed in triplicate. $*P < 0.05$.

need to simultaneously inhibit PI3K, its downstream protein, AKT, and mTOR to achieve a robust anti-cancer effect using an inhibitor like CMG002 suggests that these proteins are critical in the carcinogenic pathway of EBVaGC, adding to the novelty of our findings. We have further demonstrated that inhibition of the PI3/ATK/mTOR pathway by escalating doses of CMG002 does not promote cancer survival by shunting via the MEK/ERK pathway. This promising effect of CMG002 suggests that it may not be prone to triggering survival-promoting escape pathways in cancer cells. Finally, we demonstrate that inhibition of autophagy in these cancer cell lines using an autophagy inhibitor like CQ or bafilomycin A1 does not promote the growth potential for these cells. Rather, when used with CMG002, CQ has a synergistic cytotoxic effect, particularly against EBV-infected GC cell lines (Fig. 10).

PI3K/mTOR dual inhibitors have shown promising anti-cancer effects in GC (Bhattacharya et al., 2012; Hart et al., 2013; Zhang et al., 2013; Zhu et al., 2015). The PI3K/mTOR dual inhibitor, BEZ-235, for example, has been reported to enhance the therapeutic effects of nab-paclitaxel in GC (Zhang et al., 2013). BEZ-235 additionally demonstrated superior anti-cancer activity in HER2-positive GC than trastuzumab primarily by inhibiting the HER2 downstream signaling pathway while also promoting a synergistic interaction with trastuzumab (Zhu et al., 2015). However, to date, the reports on the optimal strategy to maximize the effectiveness of PI3K/mTOR dual inhibitors are still lacking for GC treatment. This study was designed to identify the subtype of GC that would be the best candidate for dual inhibition of PI3K/mTOR and how we might optimize efficacy of PI3K/mTOR dual inhibitors by regulating cellular autophagy.

First, we confirmed that the new PI3K/mTOR dual inhibitor, CMG002, has remarkable anti-cancer activity in EBV-infected GC cell lines. EBV has been known to play an important role in carcinogenesis by promoting cancer cell proliferation and survival through the PI3K/AKT/mTOR pathway activation (Chen et al., 2008; Shair et al., 2008; Shin et al., 2010). Up-regulated phosphorylation of AKT has been reported in the EBV-infected GC cell line, NUGC3 (Fukagawa et al., 2008). In line with these findings, our study also demonstrates an increase in phosphorylated AKT in not only EBV-infected NUGC3 cells but also in EBV-infected AGS cells when compared with mock-infected cells (Figs. 2A and 2B). CMG002 effectively blocked the PI3K/AKT/mTOR pathway in these EBV-infected cell lines by decreasing phosphorylation of AKT at much lower concentrations than its IC50 would predict (Fig. 3B). We additionally observed that CMG002 downregulated the expression of S6, a protein downstream of mTOR, a novel finding in our study, pointing to additional proteins that may be the target of our new compound. Future experiments will target the mechanism by which CMG002 directly downregulates S6. In contrast to the reports

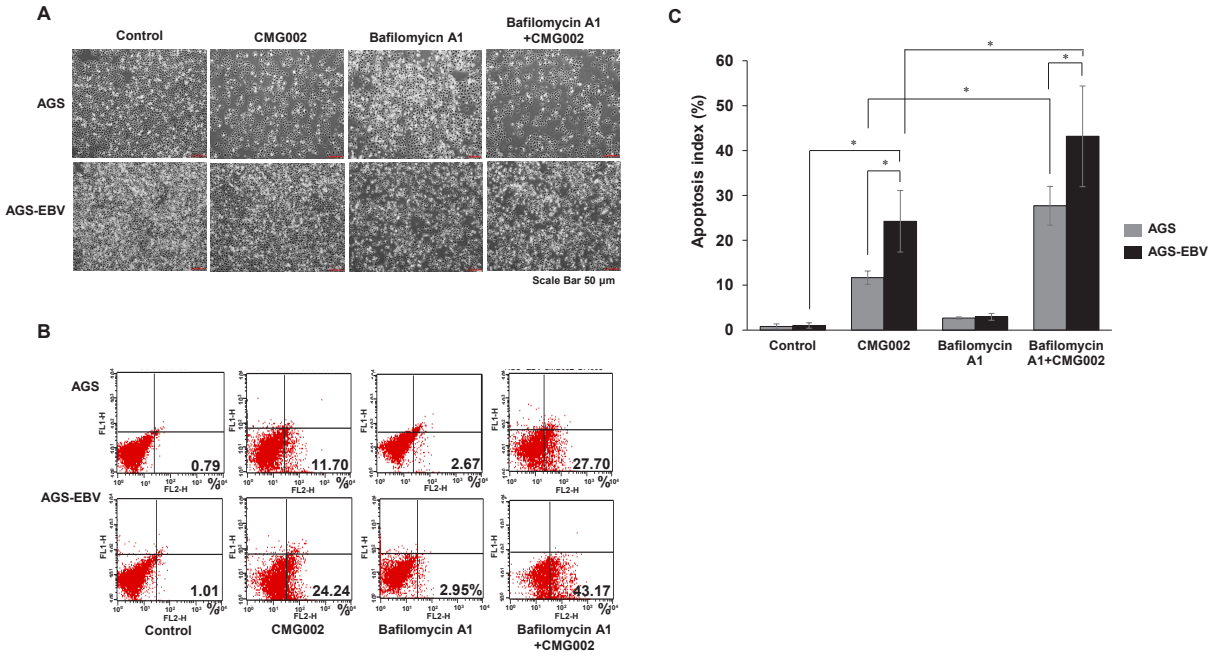

Fig. 8. Synergistic apoptotic cell death induced by SCT using bafilomycin A1 and CMG002 in AGS cell line. (A) Representative images of EBV- and mock-infected AGS cells 48 hours post-SCT with 2.5 nM of bafilomycin A1 for 1 hour followed by concomitant 2.5 nM bafilomycin and 100 nM of CMG002 for the remainder of the 48-hour period (40× magnification). (B) Flow cytometry-based TUNEL assay demonstrating gating of apoptotic cells 48 hours following monotherapy and SCT with bafilomycin A1 and CMG002. The percentage of apoptotic cells represents the mean of three or more independent experiments. (C) Apoptotic index (%) in EBV- and mock-infected AGS cells following 48 hours of treatment with monotherapy and SCT with bafilomycin A1 and CMG002. Results represent the mean ± SEM of experiments conducted in triplicate. $*P < 0.05$.

of other PI3/mTOR inhibitors such as BEZ-235, PKI-587, GDC-0980, and VS-5584 used in pancreatic cancer, we found that CMG002 did not induce a compensatory activation of MEK/ERK pathway in our GC cell lines (Supplementary Fig. S1) (Ning et al., 2017; Soares et al., 2015). We hypothesize that the differential activation of MEK/ERK pathway by PI3K/mTOR dual inhibitors may be idiosyncratic to individual inhibitors acting on specific cancer subtypes or cancer cell lines. Further studies on the mechanism by which CMG002 prevents activation of the MEK/ERK pathway are warranted to delineate these additional beneficial effects. We confirmed the therapeutic effect of CMG002 on the PI3K/AKT/mTOR signaling pathway by quantifying its effects on cell growth, cell cycle regulation and apoptotic cell death in EBV- and mock-infected AGS and NUGC3 cells. CMG002 inhibited cell proliferation by inducing G0/G1 cell cycle arrest in both cell lines irrespective of EBV infection, but the effect of CMG002 on cell cycle regulation was superior in EBV-infected AGS cells (Figs. 4C and 4D). The effect of the PI3K/mTOR dual inhibitor on apoptotic cell death was also superior in EBV-infected AGS and NUGC3 cells (Figs. 6 and 7), suggesting that EBVaGC might be a better target of the PI3K/mTOR dual inhibitor than non-EBVaGC.

We also investigated the effect of the PI3K/mTOR dual inhibitor, CMG002, in regulating autophagic pathways in GC cell lines. The mTOR pathway is known to play a crucial role as a negative regulator of autophagy, and PI3K/mTOR dual inhibitors have been reported to induce autophagy (Ji et al., 2015). We confirmed that CMG002 also induces autophagy, with the most pronounced effect in AGS cells, particularly EBV-infected AGS cells. Although NUGC3 cell lines did not exhibit significant autophagy activation by CMG002 regardless of EBV infection, likely due to high baseline autophagic activity, we were reassured to observe that SCT with CQ and CMG002 could still enhance apoptotic cell death in this cell line, especially in EBV-infected NUGC3 cells. The synergistic apoptotic cell death effect was consistently observed in both NUGC3 and AGS cells treated with SCT using CQ or bafilomycin A1 with CMG002 (Figs. 8 and 9). Although we cannot fully explain the mechanism behind why NUGC3 cells did not exhibit significant autophagy activation by CMG002, our ongoing studies are evaluating other autophagic pathways that may be differentially activated by CMG002 in both AGS and NUGC3 cells (Shimizu, 2018). Our results prove that autophagy inhibition is a promising therapeutic strategy to be considered in synergy with PI3K/mTOR dual inhibitors. There is growing evidence to support the use of PI3K/mTOR and autophagy inhibitors in combination to enhance apoptosis in other cancer cell types (Chang et al., 2013; Fei et al., 2016; Ghadimi et al., 2012; Ji et al., 2015). Our data suggest that autophagy inhibitors reduce autophagic activity which is relatively induced by PI3K/mTOR dual inhibitors in GC cell lines, thereby enhancing GC cell apoptosis (Choi et al., 2015). Our findings also suggest

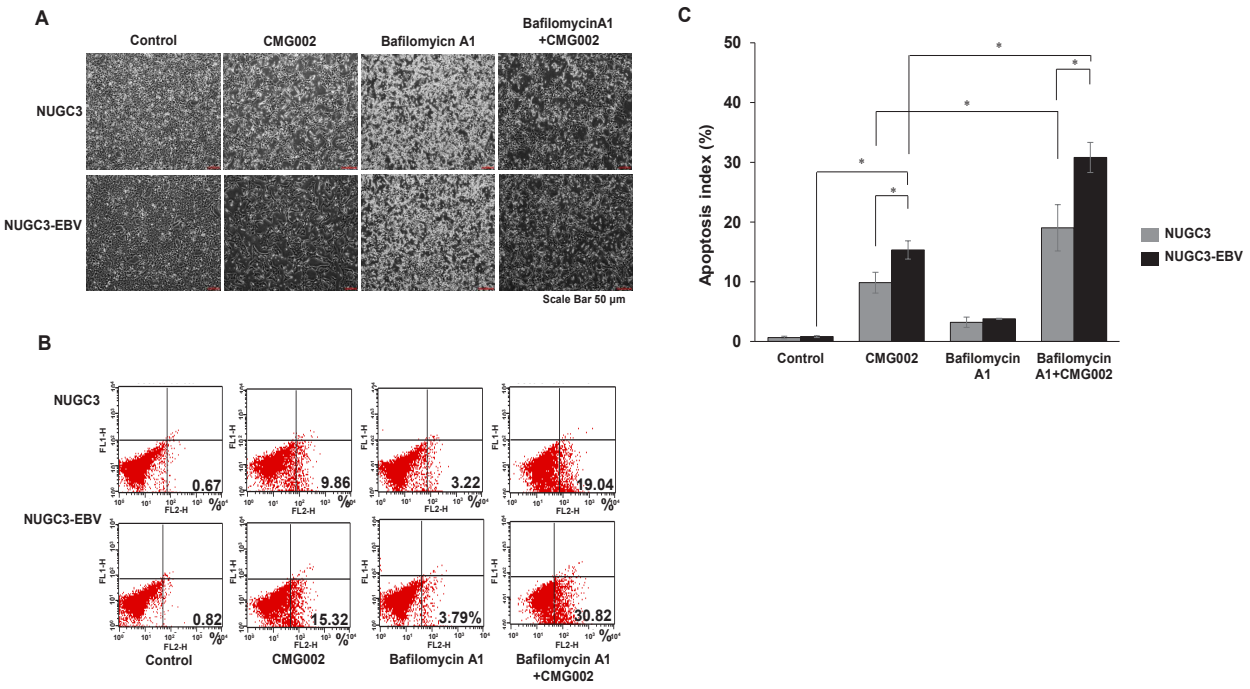

Fig. 9. Synergistic apoptotic cell death induced by SCT with bafilomycin A1 and CMG002 in NUGC3 cell line. (A) Representative images of EBV- and mock-infected NUGC3 cells 48 hours post-SCT with bafilomycin A1 and CMG002 (40× magnification). (B) Flow cytometry-based TUNEL assay demonstrating gating of apoptotic cells 48 hours following monotherapy and SCT with bafilomycin A1 and CMG002. The percentage of apoptotic cells represents the mean of more than three independent experiments. (C) Apoptotic index (%) in EBV- and mock-infected NUGC3 cells after 48 hours of treatment with monotherapy and SCT with bafilomycin A1 and CMG002. Results expressed represent the mean ± SEM from the experiments conducted in triplicate. $*P < 0.05$.

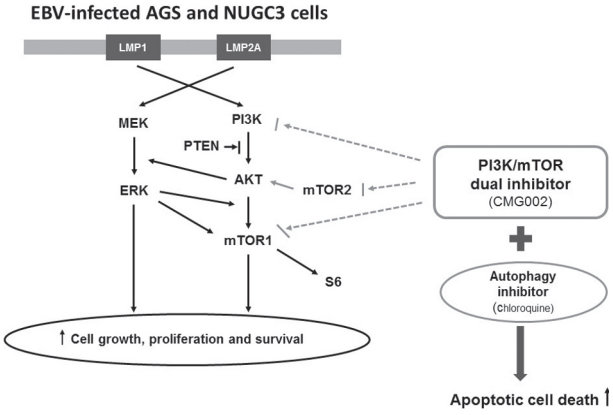

Fig. 10. Proposed schematic mechanism of EBV-associated gastric carcinogenesis via the activation of the PI3K/AKT/mTOR pathway, and its blockade by CMG002.

that both autophagy and apoptosis have an independent role in modulating cell death, and autophagic pathways may overlap with apoptotic pathways, potentially regulating apoptotic cell death in GC (Eisenberg-Lerner et al., 2009). We conclude that autophagy inhibition by CQ enhances apoptotic cell death when combined with a PI3K/mTOR dual inhibitor.

One of the limitations of our study is that we have not yet explored the mechanism behind why EBV-infected GC cell lines are particularly susceptible to apoptosis when exposed to the synergistic effects of autophagy inhibition and PI3K/mTOR dual inhibition. Our results are in line with previous reports demonstrating that autophagy inhibition enhances apoptotic cancer cell death when combined with PI3K/mTOR dual inhibitors (Chang et al., 2013; Fei et al., 2016; Ghadimi et al., 2012; Ji et al., 2015; Zhang et al., 2013), but our future studies will focus on the mechanism by which autophagy inhibition induces apoptotic cell death in EBVaGC. Second, we only utilized two autophagy inhibitors, CQ and bafilomycin A1, both of which may have multiple autophagy targets, to determine the effect of SCT in our studies. Future studies are planned with targeted genetic knockdown of autophagy regulators such as ATG7 or ATG5 and use of additional markers of autophagic flux such as autophagosome number and p62 activity (also known as SQSTM1). Lastly, additional *in vivo* experiments are needed to confirm the efficacy of CMG002 monotherapy and the combination therapy with autophagy inhibitors and CMG002 in EBVaGC.

Overall, the findings in our study not only provide evidence that the PI3K/AKT/mTOR signaling pathway is an effective therapeutic target, but give new insight into the functional role of autophagy inhibition as a mechanism to enhance apoptotic cell death in EBVaGC. We expect that our ongoing mechanistic studies and *in vivo* experiments will further

validate the therapeutic efficacy of CMG002 as a new PI3K/mTOR dual inhibitor and provide us better insights into the role of autophagy inhibition in the treatment of EBVaGC.

Note: Supplementary information is available on the Molecules and Cells website (www.molcells.org).

Disclosure
The authors have no potential conflicts of interest to disclose.

ACKNOWLEDGMENTS
CMG002 was kindly donated by CMG Pharmaceutical. We would like to thank Prof. Haengseok Song and Hye-Ryun Kim (Department of Biomedical Science, CHA University, Seongnam, Korea) for sincere comments and help on our research. Additionally, we would like to thank Jae-Hee Kim for her advice in our paper. This study was supported by a grant of the Korea Healthcare Technology R&D project, Ministry for Health, Welfare & Family Affairs, Republic of Korea (HI13C1398).

ORCID
Mi-Young Kim https://orcid.org/0000-0003-2395-5822
Annie J. Kruger https://orcid.org/0000-0001-8227-5996
Phil kyung Shin https://orcid.org/0000-0002-3935-3132

REFERENCES
Akiyama, S., Amo, H., Watanabe, T., Matsuyama, M., Sakamoto, J., Imaizumi, M., Ichihashi, H., Kondo, T., and Takagi, H. (1988). Characteristics of three human gastric cancer cell lines, NU-GC-2, NU-GC-3 and NU-GC-4. Jpn. J. Surg. *18*, 438-446.

Bhattacharya, B., Akram, M., Balasubramanian, I., Tam, K.K., Koh, K.X., Yee, M.Q., and Soong, R. (2012). Pharmacologic synergy between dual phosphoinositide-3-kinase and mammalian target of rapamycin inhibition and 5-fluorouracil in PIK3CA mutant gastric cancer cells. Cancer Biol. Ther. *13*, 34-42.

Chang, Z., Shi, G., Jin, J., Guo, H., Guo, X., Luo, F., Song, Y., and Jia, X. (2013). Dual PI3K/mTOR inhibitor NVP-BEZ235-induced apoptosis of hepatocellular carcinoma cell lines is enhanced by inhibitors of autophagy. Int. J. Mol. Med. *31*, 1449-1456.

Chen, Y.R., Liu, M.T., Chang, Y.T., Wu, C.C., Hu, C.Y., and Chen, J.Y. (2008). Epstein-Barr virus latent membrane protein 1 represses DNA repair through the PI3K/Akt/FOXO3a pathway in human epithelial cells. J. Virol. *82*, 8124-8137.

Choi, P.R., Kang, Y.J., Sung, B., Kim, J.H., Moon, H.R., Chung, H.Y., Kim, S.E., Park, M.I., Park, S.J., and Kim, N.D. (2015). MHY218-induced apoptotic cell death is enhanced by the inhibition of autophagy in AGS human gastric cancer cells. Int. J. Oncol. *47*, 563-572.

Dawson, C.W., Tramountanis, G., Eliopoulos, A.G., and Young, L.S. (2003). Epstein-Barr virus latent membrane protein 1 (LMP1) activates the phosphatidylinositol 3-kinase/Akt pathway to promote cell survival and induce actin filament remodeling. J. Biol. Chem. *278*, 3694-3704.

Eisenberg-Lerner, A., Bialik, S., Simon, H.U., and Kimchi, A. (2009). Life and death partners: apoptosis, autophagy and the cross-talk between them. Cell Death Differ. *16*, 966-975.

Fang, W.L., Huang, K.H., Lan, Y.T., Lin, C.H., Chang, S.C., Chen, M.H., Chao, Y., Lin, W.C., Lo, S.S., Li, A.F., et al. (2016). Mutations in PI3K/AKT pathway genes and amplifications of PIK3CA are associated with patterns of recurrence in gastric cancers. Oncotarget *7*, 6201-6220.

Fei, H.R., Tian, H., Zhou, X.L., Yang, M.F., Sun, B.L., Yang, X.Y., Jiao, P., and Wang, F.Z. (2016). Inhibition of autophagy enhances effects of PF-04691502 on apoptosis and DNA damage of lung cancer cells. Int. J. Biochem. Cell Biol. *78*, 52-62.

Fukagawa, Y., Nishikawa, J., Kuramitsu, Y., Iwakiri, D., Takada, K., Imai, S., Satake, M., Okamoto, T., Fujimoto, M., Okita, K., et al. (2008). Epstein-Barr virus upregulates phosphorylated heat shock protein 27 kDa in carcinoma cells using the phosphoinositide 3-kinase/Akt pathway. Electrophoresis *29*, 3192-3200.

Ghadimi, M.P., Lopez, G., Torres, K.E., Belousov, R., Young, E.D., Liu, J., Brewer, K.J., Hoffman, A., Lusby, K., Lazar, A.J., et al. (2012). Targeting the PI3K/mTOR axis, alone and in combination with autophagy blockade, for the treatment of malignant peripheral nerve sheath tumors. Mol. Cancer Ther. *11*, 1758-1769.

Hart, S., Novotny-Diermayr, V., Goh, K.C., Williams, M., Tan, Y.C., Ong, L.C., Cheong, A., Ng, B.K., Amalini, C., Madan, B., et al. (2013). VS-5584, a novel and highly selective PI3K/mTOR kinase inhibitor for the treatment of cancer. Mol. Cancer Ther. *12*, 151-161.

Hino, R., Uozaki, H., Murakami, N., Ushiku, T., Shinozaki, A., Ishikawa, S., Morikawa, T., Nakaya, T., Sakatani, T., Takada, K., et al. (2009). Activation of DNA methyltransferase 1 by EBV latent membrane protein 2A leads to promoter hypermethylation of PTEN gene in gastric carcinoma. Cancer Res. *69*, 2766-2774.

Imai, S., Nishikawa, J., and Takada, K. (1998). Cell-to-cell contact as an efficient mode of Epstein-Barr virus infection of diverse human epithelial cells. J. Virol. *72*, 4371-4378.

Ji, Y., Di, W., Yang, Q., Lu, Z., Cai, W., and Wu, J. (2015). Inhibition of autophagy increases proliferation inhibition and apoptosis induced by the PI3K/mTOR inhibitor NVP-BEZ235 in breast cancer cells. Clin. Lab. *61*, 1043-1051.

Klionsky, D.J., Abdelmohsen, K., Abe, A., Abedin, M.J., Abeliovich, H., Acevedo Arozena, A., Adachi, H., Adams, C.M., Adams, P.D., Adeli, K., et al. (2016). Guidelines for the use and interpretation of assays for monitoring autophagy (3rd edition). Autophagy *12*, 1-222.

Levine, B., and Kroemer, G. (2008). Autophagy in the pathogenesis of disease. Cell *132*, 27-42.

Liu, P., Begley, M., Michowski, W., Inuzuka, H., Ginzberg, M., Gao, D., Tsou, P., Gan, W., Papa, A., Kim, B.M., et al. (2014). Cell-cycle-regulated activation of Akt kinase by phosphorylation at its carboxyl terminus. Nature *508*, 541-545.

Mirzoeva, O.K., Hann, B., Hom, Y.K., Debnath, J., Aftab, D., Shokat, K., and Korn, W.M. (2011). Autophagy suppression promotes apoptotic cell death in response to inhibition of the PI3K-mTOR pathway in pancreatic adenocarcinoma. J. Mol. Med. (Berl.) *89*, 877-889.

Ning, C., Liang, M., Liu, S., Wang, G., Edwards, H., Xia, Y., Polin, L., Dyson, G., Taub, J.W., Mohammad, R.M., et al. (2017). Targeting ERK enhances the cytotoxic effect of the novel PI3K and mTOR dual inhibitor VS-5584 in preclinical models of pancreatic cancer. Oncotarget *8*, 44295-44311.

Samuels, Y., Wang, Z., Bardelli, A., Silliman, N., Ptak, J., Szabo, S., Yan, H., Gazdar, A., Powell, S.M., Riggins, G.J., et al. (2004). High frequency of mutations of the PIK3CA gene in human cancers. Science *304*, 554.

Shair, K.H., Schnegg, C.I., and Raab-Traub, N. (2008). EBV latent membrane protein 1 effects on plakoglobin, cell growth, and migration. Cancer Res. *68*, 6997-7005.

Shibata, D., and Weiss, L.M. (1992). Epstein-Barr virus-associated gastric adenocarcinoma. Am. J. Pathol. *140*, 769-774.

Shimizu, S. (2018). Biological roles of alternative autophagy. Mol. Cells *41*, 50-54.

Shin, J.Y., Kim, J.O., Lee, S.K., Chae, H.S., and Kang, J.H. (2010). LY294002 may overcome 5-FU resistance via down-regulation of activated p-AKT in Epstein-Barr virus-positive gastric cancer cells. BMC Cancer *10*, 425.

Soares, H.P., Ming, M., Mellon, M., Young, S.H., Han, L., Sinnet-Smith, J., and Rozengurt, E. (2015). Dual PI3K/mTOR inhibitors induce rapid overactivation of the MEK/ERK pathway in human pancreatic cancer cells through suppression of mTORC2. Mol. Cancer Ther. *14*, 1014-1023.

Zhang, C.H., Awasthi, N., Schwarz, M.A., and Schwarz, R.E. (2013). The dual PI3K/mTOR inhibitor NVP-BEZ235 enhances nab-paclitaxel antitumor response in experimental gastric cancer. Int. J. Oncol. *43*, 1627-1635.

Zhu, Y., Tian, T., Zou, J., Wang, Q., Li, Z., Li, Y., Liu, X., Dong, B., Li, N., Gao, J., et al. (2015). Dual PI3K/mTOR inhibitor BEZ235 exerts extensive antitumor activity in HER2-positive gastric cancer. BMC Cancer *15*, 894.